Understanding Concentric Split Ring Resonators and its Microwave Microplasma Properties

IEPC-2017-189

Presented at the 35th International Electric Propulsion Conference,
Georgia Institute of Technology • Atlanta, Georgia • USA
October 8 – 12, 2017

Roberto A. Dextre[1] and Kunning G. Xu[2]
University of Alabama in Huntsville, Huntsville, AL, 35806, USA

In this paper, a microwave powered microstrip concentric split ring resonator microplasma source was developed and the effect of the harmonic nested ring design on the microplasma properties was studied. The end-goal of this work is to implement the concentric split ring resonator into an in-space micropropulsion system. We thus need to understand the behavior of the microplasma to optimize the thruster performance. A single split ring resonator design was utilized for comparison. The microplasma properties from two devices were analyzed; a single split ring resonator and a concentric split ring resonator. The microplasmas were generated in argon. Simulations of the electric fields were performed to understand the electric field behavior of the concentric device. Single Langmuir probe measurements were taken at a pressure of 1 Torr to obtain the plasma density and electron temperature. Utilizing the concentric ring, the results showed a decrease in electron temperature from 8.53 eV, from the single device, to 3.13 eV. A different trend was observed for the electron density as the concentric device recorded 1.14×10^{15} /m^3 while the single device obtained 5.49×10^{14} /m^3. The microwave power was set at approximately 20 W.

I. Introduction

The study of microplasmas focuses on plasma discharges that are confined to millimeter or smaller scales. Microplasmas have a range of potential applications including bacteria sterilization[1,2], treatment of skin[3], surface activation[2], nanomaterial synthesis[4], and thin film coating.[5] A variety of configurations can be utilized for the production of microplasmas, but microstrip technology is emphasized in this paper. Microstrip technology focuses on the development of thin-stripped (34 microns) antennas on a high dielectric substrate. The shape of the antenna have been known to be linear[6] or ring[5] geometries. The configuration known as a split ring resonator (SRR) is a split ring microstrip acting as an antenna connected to a microwave source. The microwave signal travels through the ring of the microstrip to the gap where a strong electric field is formed that ionizes the surrounding gas and generates the microplasma. Previous research focused on producing microplasmas using this technology and understanding the microplasma properties[7]. Another aspect of this technology is known as concentric split ring resonator (CSRR) technology which adds a nested harmonic concentric ring to the substrate with the original powered ring. Research on CSRRs exists focusing on the inter-ring spacing[8] and the electromagnetic resonance behaviors[9]. However, the microplasma produced by a CSRR has not been studied. It is assumed that the effect of the additional harmonic rings can enhance the microplasma properties produced by the device. This is primarily due to the coupling of the microwaves from the powered ring to the nested ring, leading to an additional point for ionization. This coupling has been researched while studying linear resonator technology[10]; however, it is believed that the CSRR will have an advantage due to its geometry. This advantage occurs as the points for ionization

[1] Graduate Research Assistant, Mechanical and Aerospace Engineering, robertdextre@gmail.com.
[2] Associate Professor, Mechanical and Aerospace Engineering, gabe.xu@gmail.com.

localize around the center of the ring geometries, potentially leading to a superposition of ionizing discharge gaps working to induce an enhanced microplasma.

The microplasma properties primarily focused on is the electron temperature and plasma densities. Enhancing these properties implies more energetic electrons and a higher presence of ionization. This is represented by the increase in electron temperature and plasma densities. These enhanced microplasma properties are believed to be particularly useful when implemented into a microthruster application.

II. Experiment

A. Resonator Device Characteristics and Fabrication

The primary resonator device consists of a SRR fabricated on a RT/Duroid 6010 laminate as the substrate. A nested harmonic ring is designed concentric with this primary SRR and is fabricated on the substrate as well. The 6010 Duroid has a dielectric constant of ~10.2 and has a thin film of 34 μm thick copper cladding on both sides. The CSRR is created on one side of the substrate while the back plane is untouched. The central conductor of an SMA connector is soldered to the primary SRR (outer ring) while the grounded body is soldered to the back plane. Figure 1 shows a schematic of the concentric split ring resonator design without the SMA connector and it shows a photo of an actual concentric split ring resonator device developed and utilized for this paper.

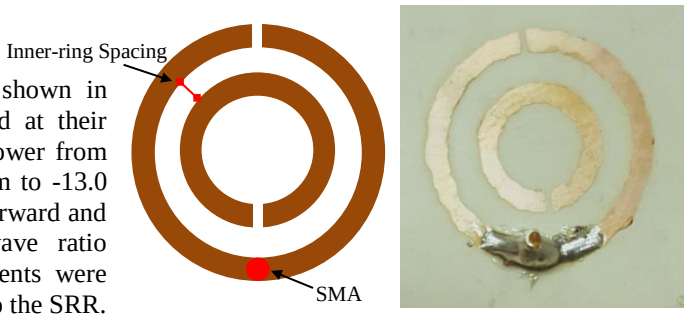

Figure 1. a) Schematic of the concentric split ring resonator with no phase angle. b) Photo of sample device.

B. Experimental Setup

A schematic of the experimental setup is shown in Figure 2. The SRR and the CSRR were tested at their resonant frequencies. The pre-amplified input power from the microwave generator ranged from -15.0 dBm to -13.0 dBm. A Bird 7020 power sensor measured the forward and reflected power and the voltage standing wave ratio (VSWR) in the circuit. The VSWR measurements were used to convert the total input power to forward to the SRR. Overall, the total forward power sent to the SRR varied from 18 W to 22 W. This power range was chosen based on the capabilities of the RF amplifier, the required ignition power, and the desire to run at < 15 W to meet small satellite power systems. All powers reported from here on is the forward power. Following the power sensor, the transmission line then enters the vacuum chamber and to the SRR. The SRRs were tested at a chamber pressure of 1 Torr-argon similar to other works. The signal then reaches the source and generates the argon microplasma.

Once the microplasma is generated, the Langmuir probe mounted near the gap was used to collect current measurements. The probe is constructed from a tungsten wire (0.127 mm diameter and a length of 2 mm), surrounded by an alumina tube. A bias voltage from -25 to 100 V is applied to the probe and current is measured. The current-voltage plot is analyzed to obtain the plasma properties.[12] A low-pass RF filter with a cutoff of 100 MHz was placed in the probe line to remove RF interference from the probe data. A Labview controlled Keithley 2410 sourcemeter was used to obtain the I-V curve. This I-V curve was generated for multiple positions mapping the microplasma properties above the discharge gap.

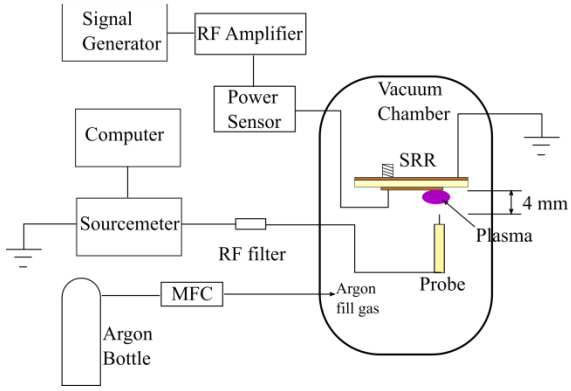

Figure 2. Diagram of the experimental setup looking at the chamber from a top-down view.

III. Results

A. Simulations

Using the ANSYS High Frequency Structure Simulator (HFSS), simulations of the single and concentric rings were determined. A 700 MHz single SRR is setup within HFSS and assigned a power of 5 W. This SRR is shown with its electric field intensity behavior from the simulation software in Figure 3a. Figure 3b shows the 700 MHz CSRR with an inner-ring spacing of 1 mm. All other geometrical characteristics of the CSRR are replicated from the SRR device. It is observed that the electric field intensity peaks at the discharge gaps of both devices within its respective ring. This includes the powered ring and the nested ring for the CSRR. Even though the outer ring geometries between the SRR and CSRR are the same, the electric field intensities of the CSRR are significantly larger than the SRR. The electric field intensity at the discharge gap for the SRR peaks at 9.07 x 10^4 V/m. For the powered ring of the CSRR, the gap electric field reached 1.43 x 10^5 V/m. The nested ring of the CSRR obtained a gap electric field intensity of 2.68 x 10^4 V/m. It is important to understand these results are generated specific to a CSRR with 1 mm inner-ring spacing. This value was chosen as it seemed to perform the best when ranging the spacing from 0.1 mm to 5 mm. At 0.1 mm, the device would have a heavy interaction along the circumference of the rings, where an even higher electric field intensity is observed from the software, yet, minimizing the power delivery to the discharge gap. This may imply that a plasma can be generated along the circumference of the ring. Closer to 5 mm, the interaction becomes minimal and the nested ring has no electric field.

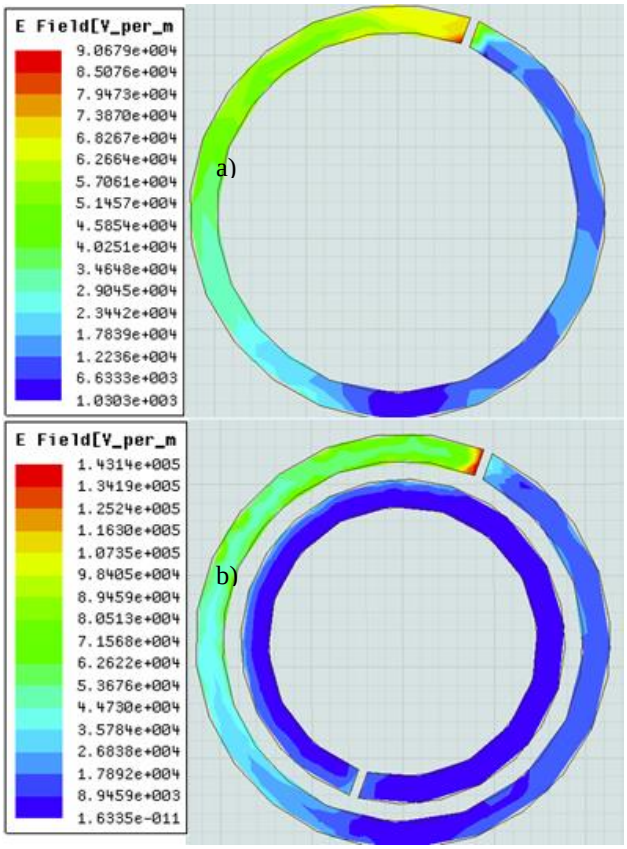

Figure 3. a) 700 MHz SRR. b) 700 MHz CSRR.

This behavior leads to the understanding that a primary factor of the coupling effect of the nested ring is its proximity to the powered ring. As the powered ring is given a microwave signal and the electric field is produced along the ring, it is known that a fringing field effect emits from the surface of the SRR[7]. Any conducting material within the fringing fields is susceptible to generating its own electric field within its structure. This defines the operation of the nested ring as it sources its power from the fringing fields of the powered ring. Once the nested ring sees this source, the field is propagated to the discharge gap as if it was its own SRR. Other research[11] agrees that the proximity coupling is likely due to the fringing electric fields from the powered ring to any sort of nearby conducting material.

The primary focus of this research is to understand the coupling effect induced by the concentric ring device. It is observed that the electric field produced in the nested ring can enhance the microplasma. The CSSR microplasma volume was visually observed to expand, but here we seek to measure the plasma properties. Single Langmuir probe measurements are used to determine the microplasma properties above the discharge gaps of each ring in both configurations. The SRR was used as a comparison to determine if the CSRR will produce higher temperatures and/or densities.

B. Single Langmuir Probe

A single Langmuir probe was used to obtain the electron temperature and plasma densities above the discharge gaps of the devices. The discharge gaps include the powered ring of both configurations and the nested ring of the CSRR.

The results are presented in Table 1. As the results show, the nested ring does impact the generated microplasma significantly. The first observation is the drop in the electron temperature. With a presence of another conducting material near the discharge gap of the powered ring, it is likely that the nested ring is also collecting current due to exposure of the microplasma. However, it seems that the population density measured by the probe picks up a higher electron and ion density for the CSRR. This increase production of particles may be justified by the operation of a secondary nested SRR. Based on physical inspection of the plasma, an increase in plasma volume is observed with the CSRR. This can be observed in the Figure 4 below.

Table 1. Comparison of plasma properties above powered ring discharge gaps of SRR and CSRR.

Plasma Property	SRR	CSRR
Electron Temperature (eV)	8.53	3.13
Plasma Potential (V)	53.49	43.45
Floating Potential (V)	23.00	-100.00
Electron Saturation Current (A)	6.9×10^{-3}	6.0×10^{-3}
Ion Saturation Current (A)	3.71×10^{-5}	3.39×10^{-5}
Electron Density ($/m^3$)	5.49×10^{14}	1.14×10^{15}
Ion Density ($/m^3$)	3.01×10^{12}	4.55×10^{12}

Figure 4 shows photos of the operating devices taken during the experiment. These microplasmas ignited at ~1 Torr with 22 W of microwave power with a resonant frequency of 787 MHz.

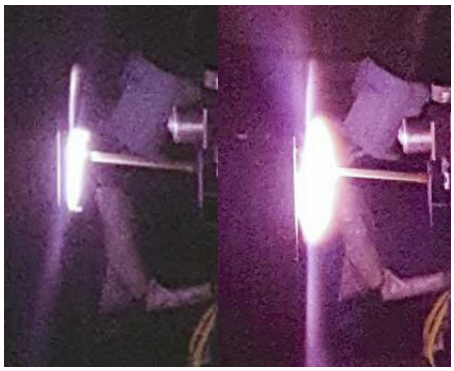

Figure 4. a) Photo of SRR. b) Photo of CSRR. Both microplasmas ignited under similar conditions.

IV. Conclusion

In this work we measured the plasma properties of a CSRR compared to an SRR. A comparison between the electron temperature and plasma density data of both configurations show increased plasma density and decreased electron temperature with the nested ring. The coupling effect of the fringing electric fields is presumed to be the primary factor for this enhancement. As the nested ring is coupled with the powered ring, it behaves as a secondary SRR based on the simulations. With a corresponding SRR acting within the powered SRR, it is possible that a secondary microplasma is ignited in response to the powered ring ignition. Future work for this research involves the utilization of a probe mapping technique that obtains microplasma property distribution data using a single Langmuir probe and a dual motion stage.

V. References

[1] Shimizu, K., Blajan, M., and Kuwabara, T., "Removal of indoor air contaminant by atmospheric microplasma," *IEEE Transactions on Industry Applications*, vol. 47, 2011, pp. 2351–2358.

[2] Mizuno, A., "Recent progress and applications of non-thermal plasma," *Int. J. Plasma Environ. Sci. Technol*, 2009, pp. 1–7.

[3] Hong, Y. C., and Uhm, H. S., "Microplasma jet at atmospheric pressure," *Applied Physics Letters*, vol. 89, 2006, pp. 2004–2007.

[4] Mariotti, D., and Sankaran, R. M., "Microplasmas for nanomaterials synthesis," *Journal of Physics D: Applied Physics*, vol. 43, 2010, p. 323001.

[5] Iza, F., and Hopwood, J., "Split-ring resonator microplasma: microwave model, plasma impedance and power efficiency," *Plasma Sources Science and Technology*, vol. 14, May 2005, pp. 397–406.

[6] Wu, C., Hoskinson, A. R., and Hopwood, J., "Stable linear plasma arrays at atmospheric pressure," *Plasma Sources Science and Technology*, vol. 20, 2011, p. 045022.

[7] Iza, F., and Hopwood, J. A., "Low-Power Microwave Plasma Source Based on a Microstrip Split-Ring Resonator," vol. 31, 2003, pp. 782–787.

[8] Castro, P. J., Barroso, J. J., and Neto, J. P. L., "Experimental Study on Split-Ring Resonators with Different Slit Widths," *Journal of Electromagnetic Analysis and Applications*, vol. 05, 2013, pp. 366–370.

[9] Gay-balmaz, P., Martin, O. J. F., and Introduction, I., "Electromagnetic resonances in individual and coupled split-ring resonators," vol. 92, 2002, pp. 2929–2936.

[10] Zhang, Z. B., and Hopwood, J., "Linear arrays of stable atmospheric pressure microplasmas," *Applied Physics Letters*, vol. 95, 2009, pp. 0–3.

[11] Hong, J., and Lancaster, M. J., "Couplings of Microstrip Square Open-Loop Resonators for Cross-Coupled Planar Microwave Filters," *IEEE Transactions on Microwave Theory and Techniques*, vol. 44, 1996, pp. 2099–2109.

[12] Dextre, R. A., and Xu, K. G., "Effect of the Split-Ring Resonator Width on the Microwave Microplasma Properties," *IEEE Transactions on Plasma Science*, vol. 45, 2017, pp. 215–222.